Available online at www.sciencedirect.com

jmr&t Journal of Materials Research and Technology

www.jmrt.com.br

Original Article

Lanthanides: a focused review of eutectic modification in hypoeutectic Al–Si alloys

*Ozen Gursoy**, *Giulio Timelli*

University of Padova, Department of Management and Engineering, Stradella S. Nicola, 3 I-36100 Vicenza, Italy

ARTICLE INFO

Article history:
Received 20 March 2020
Accepted 27 May 2020

Keywords:
Lanthanides
Rare earth
Eutectic modification
Silicon morphology
Aluminium alloy

ABSTRACT

A modified fibrous-like eutectic structure strongly improves the final mechanical properties of Al–Si foundry alloys, especially ductility. Beside widely used commercial eutectic modifiers such as Sr and Na, lanthanides appear to be a possible alternative in the eutectic Si modification process for hypoeutectic Al–Si casting alloys. All lanthanides have similar physical and chemical properties, such as density, melting point, and fading phenomena, which have been compared in the present review. They also show atomic radii close to the optimal atomic radius for a modifying agent. However, the microstructural evolution of eutectic Si is strictly related to the specific element and content of lanthanides, whose abundance, reserve, mining, production and market situations have been preliminary evaluated in this paper. The eutectic modification mechanisms induced by lanthanides are not well-discussed and clarified yet. The advantages and disadvantages of individual addition of lanthanides for chemical modification of hypoeutectic Al–Si alloys have been here critically reviewed. The use of lanthanides for eutectic Si modification in Al–Si alloys has been discussed from both effectiveness and economical point of views. Nowadays, the actual cost and their efficiency seem to make lanthanides still far to be used in foundry industry for commercial and large-scale applications.

1. Introduction

Discovery of lanthanides was taken place in a small village called “Ytterby” in Sweden on 1788. In the early years, they were called “black rock” and subsequently “new kind of earth”. Approximately 5000 t of rare earth oxide production was sufficient for the global demand before the 1950s. After that, the demand has gradually increased year by year because of the cold war, nuclear armament and space race [1,2]. Nowadays, the application of lanthanides has widened in daily life such as touchscreens, lighting products, computer technology; furthermore, lanthanides are used in medical systems, screen technology, automotive industry (especially in electric cars), defence and metallurgy industry [2,3]. Lanthanide usage in catalysts, glassmaking and metallurgy markets, called also mature markets, accounts for 52% of the total worldwide market demand; permanent magnet, ceramic and battery markets, nominally high-growth markets, are the remainder of the market demand [4].

* *Corresponding author.*
E-mails: yozen.gyursoy@phd.unipd.it (O. Gursoy), timelli@gest.unipd.it (G. Timelli).
https://doi.org/10.1016/j.jmrt.2020.05.105

In the mature market, including metallurgy, lanthanum, cerium and neodymium elements constitute 83% of rare earth (RE) demand of the market itself. In metallurgy industry, lanthanides are added into aluminium, magnesium and iron-based alloys in small quantities in the form of master alloys or mischmetal, i.e. mostly La and/or Ce based RE mixture, to mainly improve the mechanical performance of the alloys. About 11,300 t rare earth oxide (REO) was used in 2018 [4].

Aluminium–silicon alloys are used in the automotive and aerospace sectors due to their high strength-to-weight ratio. Preliminary molten metal treatments, such as grain refinement and eutectic modification, are generally performed through the addition of some elements in the molten bath in order to improve the mechanical properties such as ductility and fatigue life. In particular, the eutectic modification in the Al–Si system has been studied by using different elements in the periodic table to achieve the best eutectic silicon modification [5]. Although sodium and strontium remain well known eutectic Si modifiers, having low prices and high availability in the market, they have shown negative or insufficient effects. Therefore, lanthanides are the current research topic despite their high prices.

In this review, the effects of the addition of individual lanthanide element on the eutectic modification in hypoeutectic Al–Si alloys are surveyed and future opportunities are discussed.

2. Lanthanides as a term

Lanthanides consist fifteen elements from lanthanum to lutetium (atomic number: 57–71) in group IIIB of the periodic table. They have chemical and physical uniformity resulting from the nature of electronic configurations. Their oxidation states are stable and equal to +3. Lanthanide-group elements have the ability to make strong ionic bonding owing to their being electropositive.

In general, lanthanides are called rare earth elements. Yttrium and scandium are extracted from the same ores in nature. Lanthanons term (abbr. Ln) comprises sixteen elements: lanthanides plus yttrium. Scandium, the lightest element in the group IIIB, has relatively noticeable chemistry because of its relatively low 3+ ion radius.

Light rare earth elements, i.e. from La to Sm, constitute approximately 98% of all rare earth ores; heavy rare earth elements, from Eu to Lu, constitute the remainder. In addition, another classification of these elements defines as middle rare earth elements those from Pm to Ho [6,7]. Fig. 1 shows the abundance of elements in the Earth's crust. Lanthanides constitute 0.02 wt.% of the Earth's entire crust, while aluminium and strontium constitute 8.6 wt.% and 0.037 wt.%, respectively. Also, pie chart shows the detailed percentage distribution of lanthanides. Cerium, the most common rare earth metal, constitutes 36 wt.% of all lanthanides. Thulium, lutetium, terbium, and holmium are quite rare. Promethium that can be produced in a nuclear reactor is rare with about 500 g occurring naturally in the crust [7,8]; due to this, promethium will not be considered in this review.

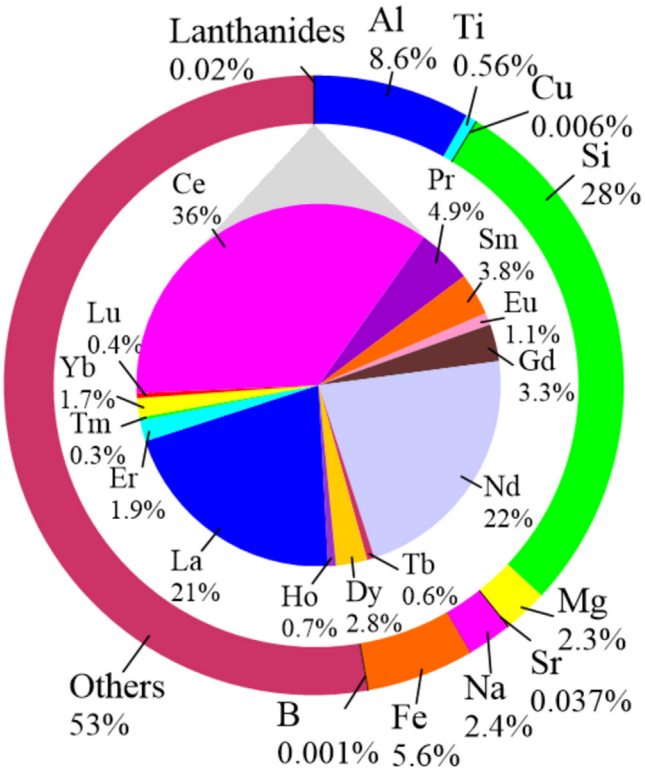

Fig. 1 – The doughnut chart (outer chart) shows abundance of the principal metals in the Earth's crust; a detailed distribution of lanthanides is shown in the pie chart (inner chart).
Data (in wt.%) refer to 2015 and are all elaborated from Ref. [8].

3. Production and market of lanthanides

Although lanthanides are distributed around the world, their ores are mainly extracted in China. Milling, floating, separation, and purification processes are carried out in China as well. This country shows a strategic position in rare earth production and market in the world [3,9]. According to the production and reserve data of 2018 (Fig. 2), the world's total rare earth reserve is 120 million t. China retains 37% of these reserves and dominates the REO production. The REO production amount of China for 2018 was 120,000 t. Australia was in second place with 20,000 t of REO [10].

World REO production has shown an increasing tendency driven by China until 2010. Global financial crisis affected the production from 2010 to 2013 (see Fig. 3). The trend has started increasing again from 2013 again. Simultaneously with the worldwide financial crisis, commercial tensions between China and Japan resulted in China's cessation of rare-earth trade to Japan on 2010. The prices of metallic lanthanide have been strictly affected by the aforementioned crises as can be seen in Fig. 4: the lanthanide prices decreased after 2010. Thus, the importance of lanthanides and their domestic production have been progressively understood in the rest of the world too. Fig. 3 evidences really the increasing world production of REO respect to that of China.

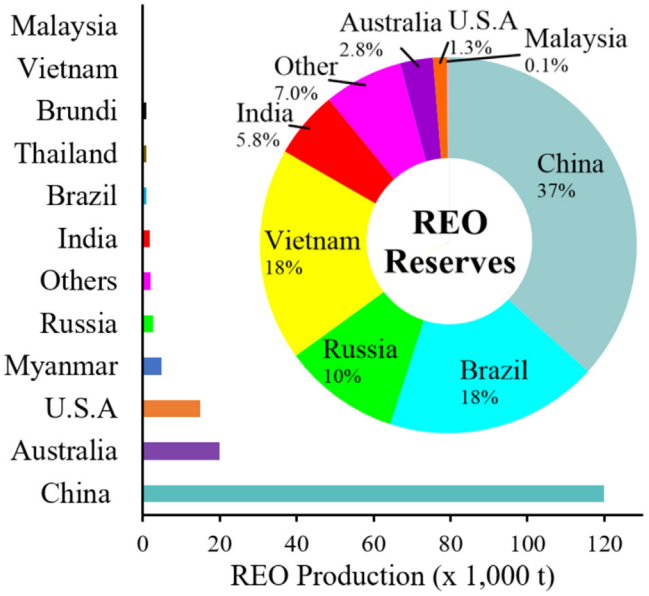

Fig. 2 – Doughnut chart shows the percentage of rare earth oxide (REO) reserves by countries. The bar chart shows the amount of REO production by countries.
Data refer to 2018 and are all elaborated from Ref. [10].

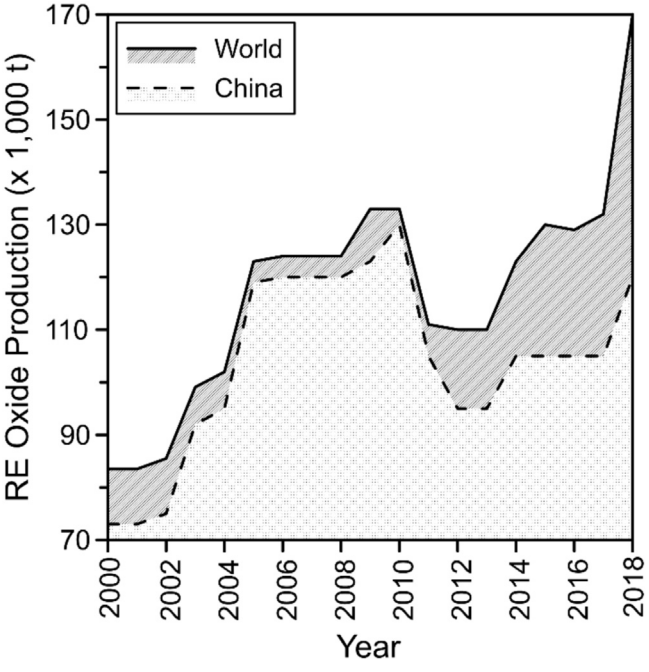

Fig. 3 – World production of rare earth oxide (REO) from 2000 to 2018, and the production in China.
Data elaborated from Ref. [10].

In 2018, the global rare earth production in oxide form was about 170,000 t (120,000 t produced in China); as useful comparison, about 60 million t of aluminium and 21 million t of copper were produced worldwide at the same time [10].

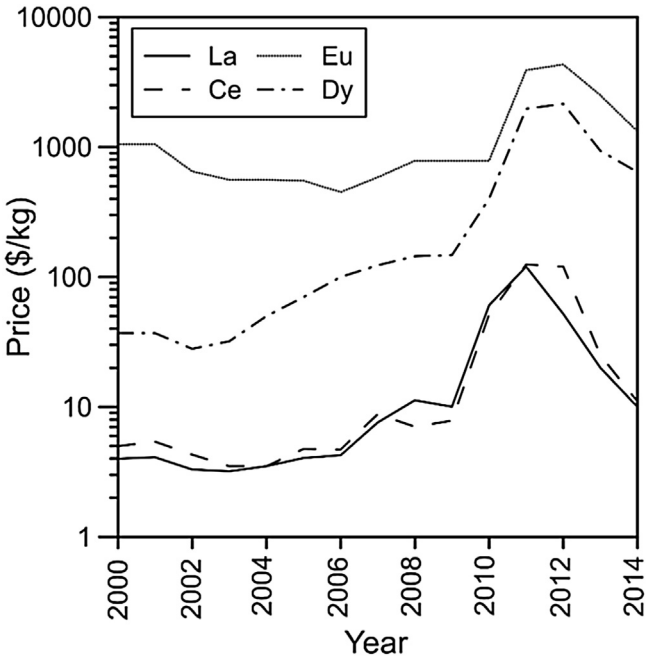

Fig. 4 – Variation in the prices of commercial purity (99.9%) lanthanum, cerium, europium and dysprosium from 2001 to 2014.
Data elaborated from Refs. [11–13].

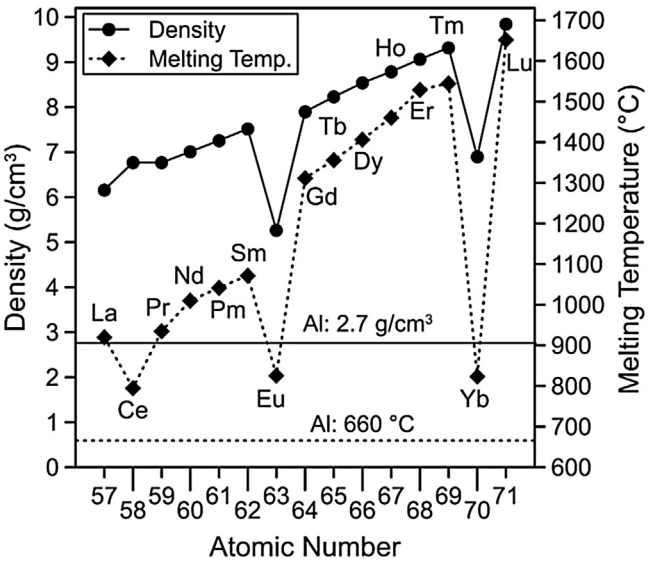

Fig. 5 – Density and melting temperature of lanthanides.
Data elaborated from Refs. [8,14].

4. Physical and chemical characteristics of lanthanides

There is an increasing trend of density and melting temperature of lanthanides with the increasing atomic number from lanthanum to lutetium. However, Fig. 5 evidences how europium and ytterbium interrupt this trend showing densities of 5.26 and 6.90 g/cm^3, respectively. Europium has the

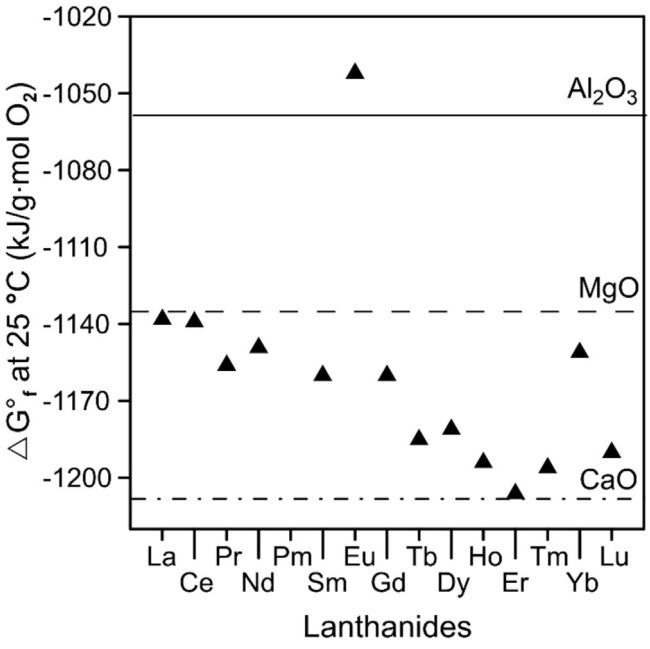

Fig. 6 – Gibbs energy for oxide formation of lanthanides; Al_2O_3, MgO and CaO are added as references. Data elaborated from Refs. [15,16].

lowest density among lanthanides, while lutetium shows the highest one, i.e. 9.84 g/cm^3. Lanthanides have a significant difference in terms of density with aluminium. Melting temperatures of lanthanides are higher than 900 °C except cerium, europium and ytterbium (795, 826 and 824 °C, respectively) [8,14].

All lanthanides have higher density (Fig. 5) and greater oxidation tendency (Fig. 6) than aluminium; both these features indicate how fading may be observed during melting process. The density difference between lanthanides and aluminium may result in the segregation of lanthanide particles at the bottom of the bath shortly after the addition. Further, greater oxidation tendency implies greater amounts of oxide occurring during the casting process.

Table 1 summarizes some physical, chemical and crystallographic properties of lanthanides, where it seems evident how europium and ytterbium are the only two elements with cubic structure. Therefore, these two elements seem to be candidates as eutectic silicon modifier in Al–Si foundry alloys.

5. The eutectic in the Al–Si system

In general, Al and Si contain impurities such as P and Fe, which can be acceptable as trace contents in commercial alloys. However, some studies [25–28] revealed how these impurities can be quite effective during the formation of Al–Si eutectic structure. According to Shankar et al. [29], the precipitation of primary α-Al from the liquid phase is followed by the formation of secondary β-Al_5FeSi phase at temperature above the eutectic point. The eutectic Si can nucleate on the β-Al_5FeSi phase before the eutectic α-Al nucleation on the Si particle.

On the other side, researchers [30,31] demonstrated that pre-existing AlP compounds in the melt play important role as effective nuclei for eutectic silicon (Fig. 7). P impurity exists as AlP compound in Al–Si alloys and it is quite effective for nucleation of silicon because of their crystallographic similarity between them. These results supported the theory from Ho and Cantor [25]: even at low P level (<2 ppm), the eutectic Si particles nucleate on AlP compounds.

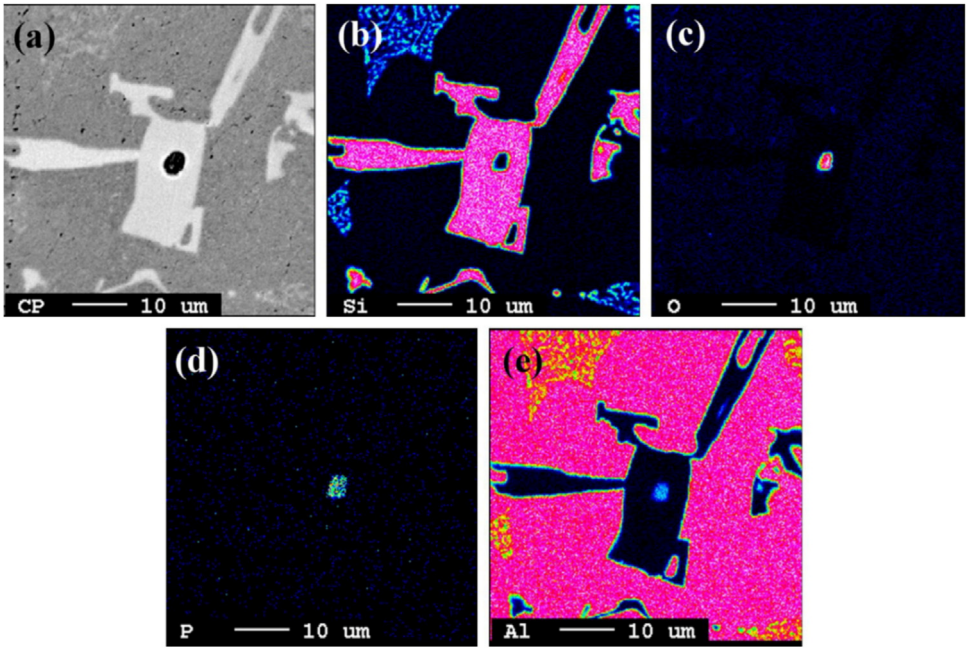

Fig. 7 – (a) Backscattered SEM micrograph showing a polyhedral silicon crystal in quenched solidified Al–7Si alloy with corresponding WDS composition maps of (b) Si, (c) O, (d) P and (e) Al. Reproduced with permission from Ref. [31]. Copyright (2014), Elsevier.

Table 1 – Some physical, chemical and crystallographic properties of lanthanides. Data elaborated from [14,17–24].

Element	Symbol	Atomic number	Crystal structure	Eutectic temperature in Al system (°C)	Eutectic point in Al system (wt.%)	Eutectic phase with α-Al
Lanthanum	La	57	DHCP[a]	640	14	$Al_{11}La_3$
Cerium	Ce	58	DHCP	640	18	$Al_{11}Ce_3$
Praseodymium	Pr	59	DHCP	640	21	$Al_{11}Pr_3$
Neodymium	Nd	60	DHCP	632	12	$Al_{11}Nd_3$
Samarium	Sm	62	Rhom.[b]	635	19	Al_3Sm
Europium	Eu	63	BCC[c]	628	11	Al_4Eu
Gadolinium	Gd	64	HCP[d]	634	16	Al_3Gd
Terbium	Tb	65	HCP	634	20	Al_3Tb
Dysprosium	Dy	66	HCP	635	16	Al_3Dy
Holmium	Ho	67	HCP	650	10	Al_3Ho
Erbium	Er	68	HCP	649	11	Al_3Er
Thulium	Tm	69	HCP	645	10	Al_3Tm
Ytterbium	Yb	70	FCC[e]	625	21	Al_3Yb
Lutetium	Lu	71	HCP	650	11	Al_3Lu

[a] Double hexagonal close-packed.
[b] Rhombohedral.
[c] Body-centred cubic.
[d] Hexagonal close-packed.
[e] Face-centred cubic.

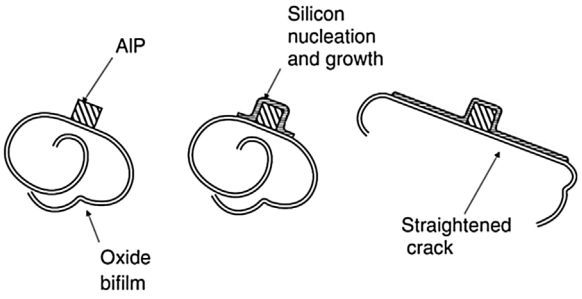

Fig. 8 – Illustration showing the nucleation of AlP particle over an oxide bifilm, which is straightened by further nucleation and growth of silicon particle. Reproduced with permission from Ref. [34]. Copyright (2015), Elsevier.

Campbell and Tiryakioglu [32,33] claimed that AlP particles nucleate on Al oxide bifilms and the eutectic Si, nucleated on AlP phase, grows on the oxide bifilm substrate (Fig. 8). Shape of planar Si particles and low mechanical behaviour of unmodified eutectic structure might be explained with straightened bifilm theory [32,33].

5.1. *Eutectic silicon modification*

The modification of Al–Si eutectic is a process that is generally applied to refine and morphologically change the eutectic Si particles leading to better performance of Al–Si cast parts [35–37]. In general, there are two different eutectic modification methods: quench modification and chemical modification. At high cooling rates, quench modification takes place intrinsically in case of an equivalent growth rate higher than 500 μm/s. The transition from flake to fibrous structure is coupled with a decrease in undercooling. The faceted silicon formation changes to non-faceted one without a significant variation in the twin density [36].

For chemical modification (also called impurity modification), a modifying agent is needed especially in some foundry processes that show low cooling rates such as sand casting. From 1921, alkali, alkaline earth metals, group VA elements, some transition metals, and lanthanides have been used or reported as useful elements for the chemical modification in Al–Si alloys [38]. The primary α-Al phase is not directly affected by impurity modification [35].

Lu and Hellawell [35] suggested two mechanisms to explain the eutectic Si modification: (1) impurity induced twinning (IIT) and (2) twin plane re-entrant edge (TPRE). In the IIT mechanism, modifier atoms or clusters are absorbed in the solute field ahead of the silicon phase at the solid/liquid interface resulting in higher twinning density. In TPRE, the branched Si structure occurs because of changed growth direction after preventing further attachment of silicon atoms into the growing structure by absorbed clusters at the re-entrant edges. Each defect is a potential site for branching during solidification in modified eutectic silicon. According to the IIT mechanism, only the elements that shows the "ideal" atomic radius ratio $r_i/r \sim 1.646$ (where r_i is the atomic radius of the element, and r is that of the silicon) are modifiers. Fig. 9 shows a plot of relative atomic radii versus the atomic radius of silicon for lanthanides.

Recently, advanced characterization techniques allowed to deeper understand the growth change of eutectic silicon when small concentrations of modifying elements are added to hypoeutectic Al–Si alloys. While light optical microscopy, electron backscattered diffraction (EBSD) and scanning electron microscopy (SEM) can provide useful information about the change in morphology and microscopic growth direction of eutectic Si, the analysis of nano sized segregations producing this effect, requires characterization methods with sub-nanometre resolution such as high-resolution transmission

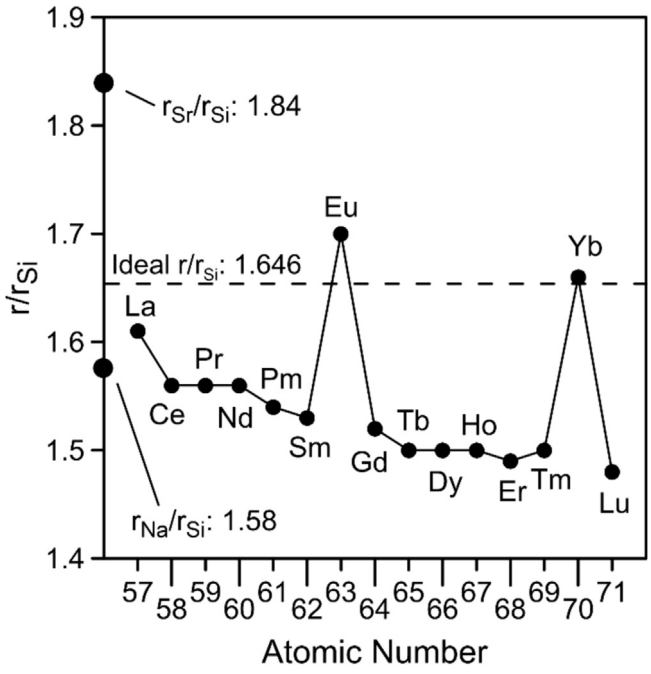

Fig. 9 – Plot of ratio of atomic radii (*r*) vs atomic radius of silicon (r_{Si}) for lanthanides; Na and Sr are indicated too. Data elaborated from Refs. [8,35].

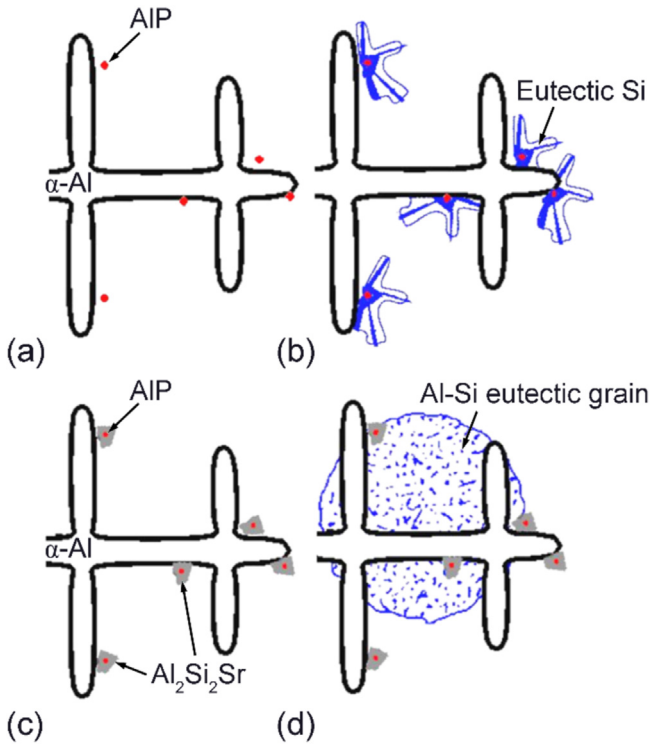

Fig. 10 – Solidification sequence of Al–Si eutectic in (a and b) unmodified and (c and d) Sr-modified alloys. Reproduced with permission from Ref. [44]. Copyright (2002), Stuart D. McDonald.

electron microscopy (HR-TEM) and atom probe tomography (APT) [39].

5.2. *Commercial eutectic Si modifiers: Na and Sr*

Two main theories are discussed in literature about the modification mechanism: (1) restricted nucleation and (2) restricted growth theories [40]. In the first one, modifier neutralizes the AlP or reduces the diffusion coefficient of Si in Al–Si melt, which results in enhanced undercooling and refined eutectic structure [41]. In the restricted growth mechanism, the preferentially absorption of modifier occurs on twin re-entrant groove or Si growing surfaces [42]. Thus, the growth of eutectic Si phase is restricted, and the eutectic structure is modified. On the other hand, Nogita et al. [43] proposed three nucleation scenarios for the Al–Si eutectic: nucleation and growth opposite the thermal gradient (Mode I), nucleation on the dendrites (Mode II) and heterogeneous nucleation of eutectic grains in the interdendritic liquid (Mode III). For chemically unmodified Al–Si alloys, the eutectic solidification occurs in Mode II, while chemically modified alloys show a development of eutectic structure through Mode III or combination of Mode I and III.

Sodium addition, discovered by Pacz in 1921, is still among the most used modification technique for hypoeutectic Al–Si alloys with high Si contents used in sand casting processes [38]. A fully eutectic modification can be achieved by a small amount of Na (<0.01 wt.%) addition [27,28,40]. Despite its excellent performance and lower price, many negative properties of Na, such as very high vapor pressure, easy evaporation, therefore quickly fading, make using Sr attractive in casting applications [35].

In unmodified alloys, AlP compounds segregate at the dendrite/liquid interface and act as nucleation sites for eutectic Si during the growth of α-Al dendrite (Fig. 10a and b). In modified alloys, low Sr levels can poison, in a similar way to Na, the AlP particles by forming Al_2Si_2Sr intermetallics which cover AlP compounds. Nucleation density decreases dramatically in the interdendritic zone and Si nucleation is forced at larger undercooling, as illustrated in Fig. 10c and d [44].

Some works [40,45] determined the absorption of Na and Sr atoms along <1 1 2> growth direction and {1 1 1} growth planes of eutectic Si. Furthermore, Si twin density in Na-modified hypoeutectic Al–Si alloys is much higher than in unmodified or Sr-modified ones, as visible in Fig. 11 [46]. The combination of Na and Sr does not result in any beneficial or synergic effect even in short period after addition [47]. Sodium dominates the eutectic solidification and increases the evaporation and fading of Sr.

5.3. *Lanthanides as eutectic Silicon modifiers*

All lanthanides have eutectic transformation in Al-rich side of their binary system, and this reaction occurs between 11 and 25 wt.% of lanthanides' addition at about 640 °C (see Table 1). Fig. 12 shows the Al–La system as example. La, Ce, Pr and Nd form a L_3Al_{11} type compound (L is lanthanide) as eutectic phase with α-Al. The other lanthanides form a LAl_3 phase, except Eu which reacts with Al and leads to an $EuAl_4$ phase.

Until now, few and partial experimental and theoretical studies on Al–Si–L ternary systems have been performed

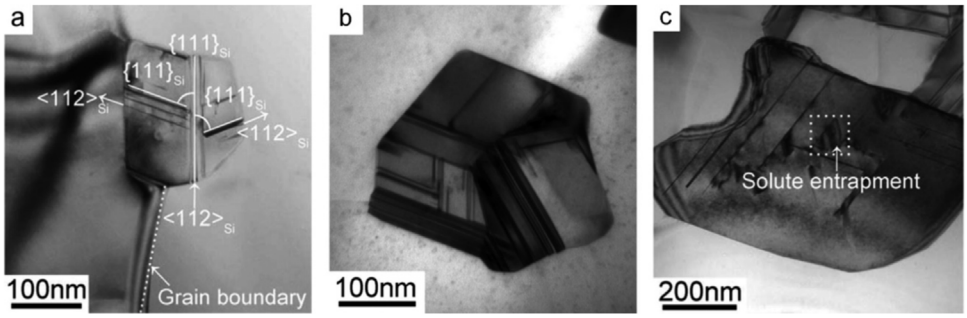

Fig. 11 – TEM bright-field images of (a) unmodified, (b) Na- and (c) Sr-modified Al–5Si alloy. Reproduced with permission from Ref. [46]. Copyright (2015), Elsevier.

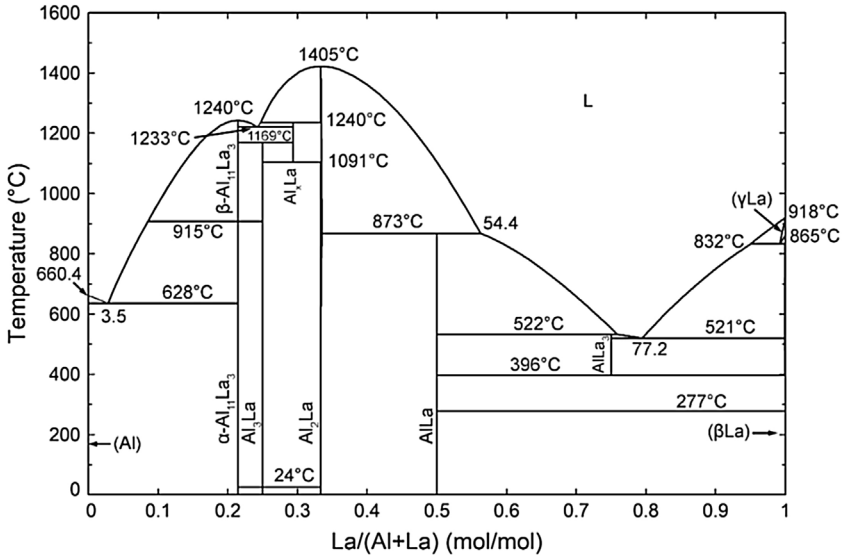

Fig. 12 – Equilibrium Al–La phase diagram calculated by the FactSage Education software.

[48–53]. However, from these preliminary works, it has been observed how lanthanides can form $Al_xSi_yL_z$-type compounds, or even more Al_2Si_2L phases, in a similar way to Sr modification. This would suggest a poisoning mechanism of the AlP particles as observed during both Na and Sr modification.

5.3.1. *Lanthanum, cerium and samarium*

New aluminium alloys containing La, Ce or Sm have been recently developed and patented [54–59]. Some authors [60–64] reported that even 1 wt.% La or Ce addition is not enough for full modification of eutectic Si. Compared to Sr modification, Ce-containing alloys show a partially modified microstructure as shown in Fig. 13 [60], where Ce-rich intermetallics (Al_2Si_2Ce phase), flake-like, and fibre-like eutectic Si particles can be easily compared. On the other hand, it is stated that good modification and twinning can be observed after 0.3 wt.% Ce addition in Al–7Si alloys. The eutectic cells nucleate at outer surface and grow inwardly [65,66]. Additionally, lanthanide element is quite effective on porosity formation, as well as the amount of addition. As seen in Fig. 6, Gibbs energy for oxide formation of Ce is slightly lower than that of La. After oxide formation, Ce is more stable than La as oxide. Thus, Ce shows greater effect on porosity formation if compared to La, and thus be more detrimental than La [67]. This can be associated to a change in the eutectic solidification. However, more efforts have to be paid to understand the mechanism of the porosity formation with addition of La, Ce or the other lanthanides.

The best efficiency of Sm addition on eutectic Si modification is reached at 0.6 wt.% in Al–12Si alloys. Furthermore, this level seems the optimum solution for Al–7Si alloys too [68,69]. Therefore, a fine-fibrous silicon morphology can be achieved by Sm addition in agreement with the IIT mechanism proposed by Lu et al. [35].

5.3.2. *Europium*

Mao et al. [70] suggested that the eutectic Si modification with Eu addition is associated with IIT and TPRE mechanisms being supported by X-ray fluorescence (μ-XRF) and X-ray absorption fine structure (XAFS) results. Eu-rich clusters were, however, detected at the {1 1 1} Si twin intersection along the <1 1 2> eutectic Si growth direction (Fig. 14) [71]. Therefore, besides TPRE and IIT mechanisms, the adsorption of modifier element into the growth interface plays a key role during the eutectic Si modification. μ-XRF and XAFS results showed a strong bonding between Eu and Si [20,71].

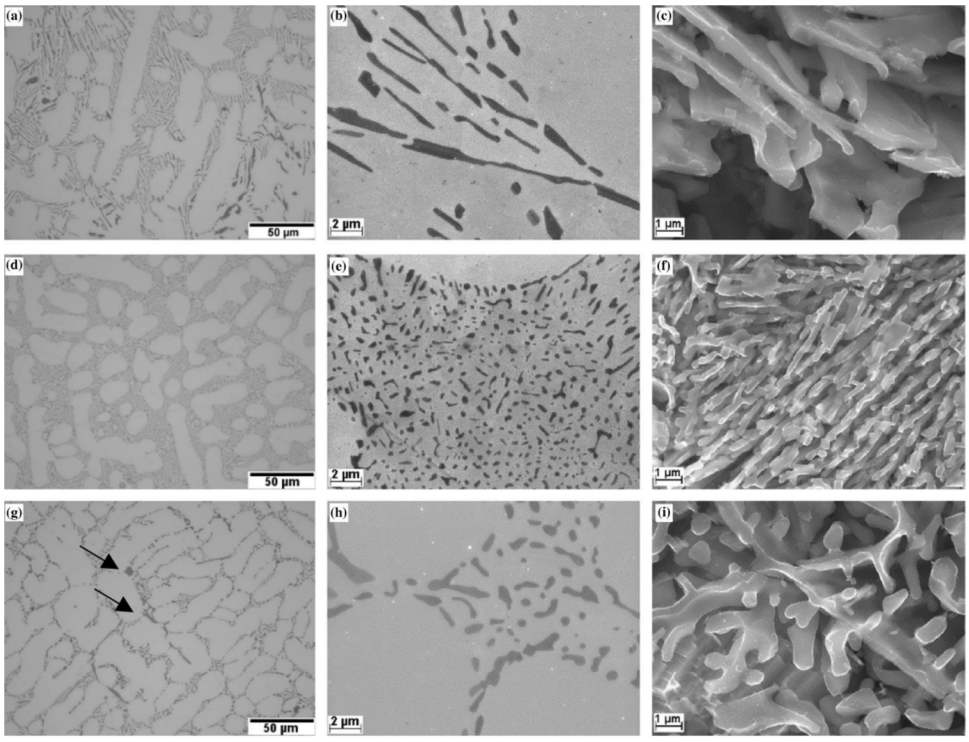

Fig. 13 – Microstructures of Al–8Si alloy (a–c) before and after (d–f) 0.04 wt.% Sr or (g–i) 1 wt.% Ce additions. (a, d, g) Optical micrographs; SEM images of (b, e, h) unetched and (c, f, h) deep etched samples. Al_2Si_2Ce particles are indicated by arrows. Reproduced with permission from Ref. [60] Copyright (2019), Springer.

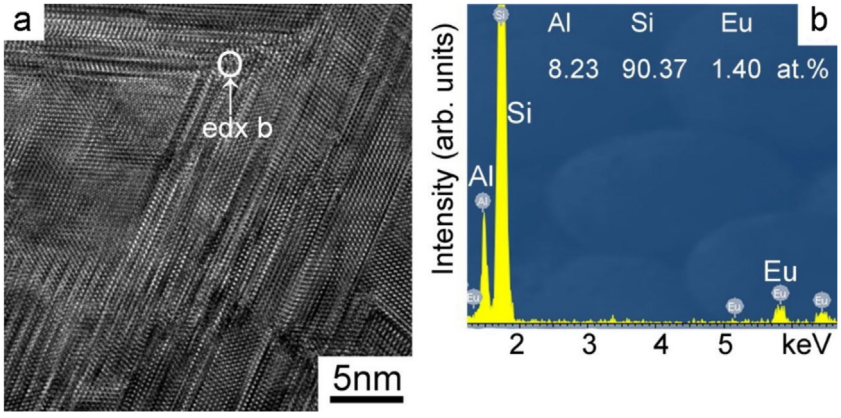

Fig. 14 – (a) High-resolution TEM image acquired along the <1 1 2>$_{Si}$ growth direction and {1 1 1}$_{Si}$ habit plane in an Al–5Si alloy after 0.05 wt.% Eu addition; (b) EDS analysis of Eu segregation at the intersection of two twins. Reproduced with permission from Ref. [71]. Copyright (2015), Elsevier.

At high levels, Eu segregates at the interface between Si and liquid during solidification. Li et al. [72] found that the modification efficiency of Eu is decreased with increasing P level in the alloy. When the P content increases up to 10 ppm, even 200 ppm Eu is not effective to reduce nucleation and growth temperatures of eutectic; however, this Eu amount is quite effective to reduce the number of eutectic grains.

There is an interaction between Eu and P resulting in EuP formation. From a crystallographic point of view, the EuP phase is a perfect nucleation site for Si particles. This may explain the refinement mechanism of eutectic Si in Eu-modified alloys.

5.3.3. *Gadolinium*

Shi et al. [73] observed a good modification degree in Gd-containing Al–7Si–0.45Mg alloy when the Gd content is about 0.4 wt.%. At lower Gd amounts (0.2 wt.%), a slight eutectic Si refinement is obtained [74]. There is no difference in the twin density of the silicon phase between unmodified and Gd-modified alloys.

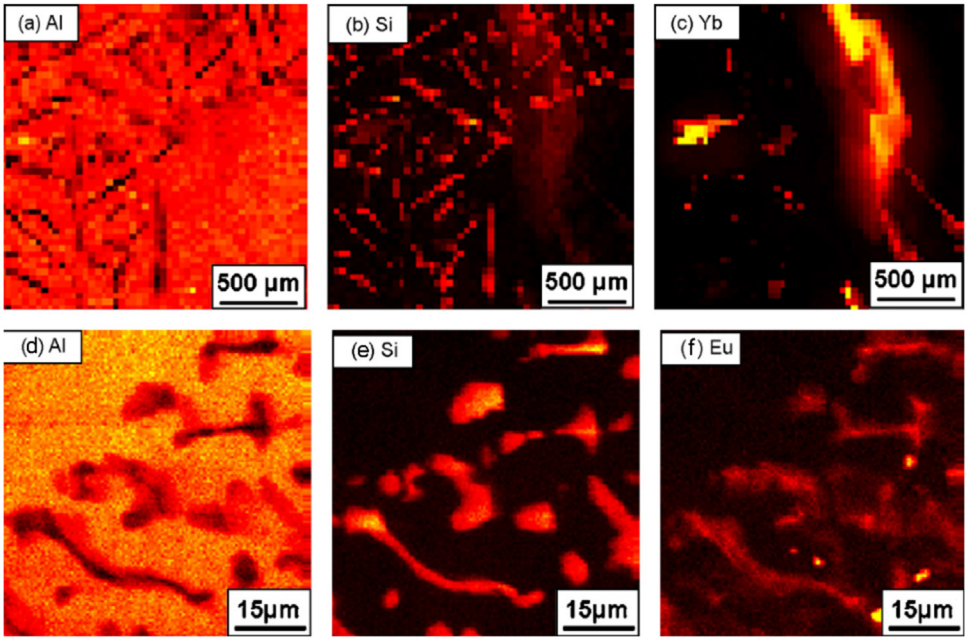

Fig. 15 – µ-XRF elemental mappings of (a–c) Eu- and (d–f) Yb-containing Al–10Si alloy. Reproduced with permission from Ref. [20]. Copyright (2010), Elsevier.

Comparing to Sr, gadolinium has smaller atomic radius and higher atomic weight. In general, the segregation of Gd atoms in front of the eutectic cell is favoured; this can lead to an eutectic refinement during solidification. Moreover, Gd has more physicochemical activity respect to Sr, La and Ce for the elimination of oxide bifilms [73]. In this way, the addition of Gd contributes to a cleaner bath, and thus greater reliability of castings.

5.3.4. *Holmium and erbium*

A high modification level can be achieved with 0.3 wt.% Ho addition in Al–7Si–0.45Mg alloy. The existence of holmium in the molten metal seems to promote the distortion of Si crystal and disturb the inherent growth orientation [75]. Greater Ho additions are not more effective for eutectic modification.

Recent studies [76–79] have shown that the optimum modification can be achieved after 0.3 wt.% Er addition into A356 alloy. More erbium is needed when the initial Si content increases; however, the modification level does not improve linearly with increasing Er concentration. It is believed that Er atoms are adsorbed along the <1 1 2> growth direction of eutectic Si being responsible for IIT and TPRE mechanisms; however, Er atoms have not been observed along with Si twins or twins' intersections [77–80].

5.3.5. *Ytterbium*

It is reported that 0.7 wt.% of Yb is needed for optimum eutectic modification in Al–10Si alloys [81,82]. Although increasing Yb up to optimum level provides better modification, no change in twin density is observed in eutectic Si particles. Li et al. [83] indicated that the depression of the eutectic temperature observed in Yb-containing alloys is not directly associated to variations in the Si morphology. This modification mechanism caused by undercooling is different from the IIT and TPRE mechanisms. Differently from Sr and Eu, Yb does not concentrate in the eutectic Si but precipitates independently in the form of Al_2Si_2Yb compounds as observed by µ-XRF mapping in Fig. 15a–c [20]. On the other side, Eu is retained in eutectic Si particles (Fig. 15d–f) [20].

5.4. *General observations and discussion*

Although Na modification is not affected by cooling rate during solidification when Na amount is high enough in the melt (>100 ppm) [40,84], lanthanides are more effective on eutectic Si modification at higher cooling rates [81,85], as generally observed in Sr-modified alloys [86].

On the other hand, increasing of lanthanide content is associated with an increase in porosity respect to unmodified alloys but also a redistribution of porosity from isolated coarse porosity to well-dispersed and fine porosity [67,72,87]. When the amount of lanthanide exceeds 1 wt.%, the porosity can form due to lanthanide-rich complex oxides and acicular or plate-like lanthanide-rich compounds, which might hinder the liquid flow during solidification [67,76,88–90].

Nogita et al. [91,92] studied the eutectic Si modification in Al–10Si alloy through high amounts (>1 wt.%) of lanthanide additions (Fig. 16). It seems lanthanides can only provide a partial eutectic modification apart from europium, which is the only lanthanide to bring about fully modification. The modification effect does not improve linearly with lanthanide addition. This is possibly due to the overcoming of lanthanide solubility, which causes the formation of precipitates, even primary compounds, which can seriously compromise the mechanical properties of the alloy in both as-cast and heat-treated conditions [93], especially ductility. Over than 1 wt.% lanthanide addition, a large number of lanthanide-rich intermetallics precipitate, and the volume

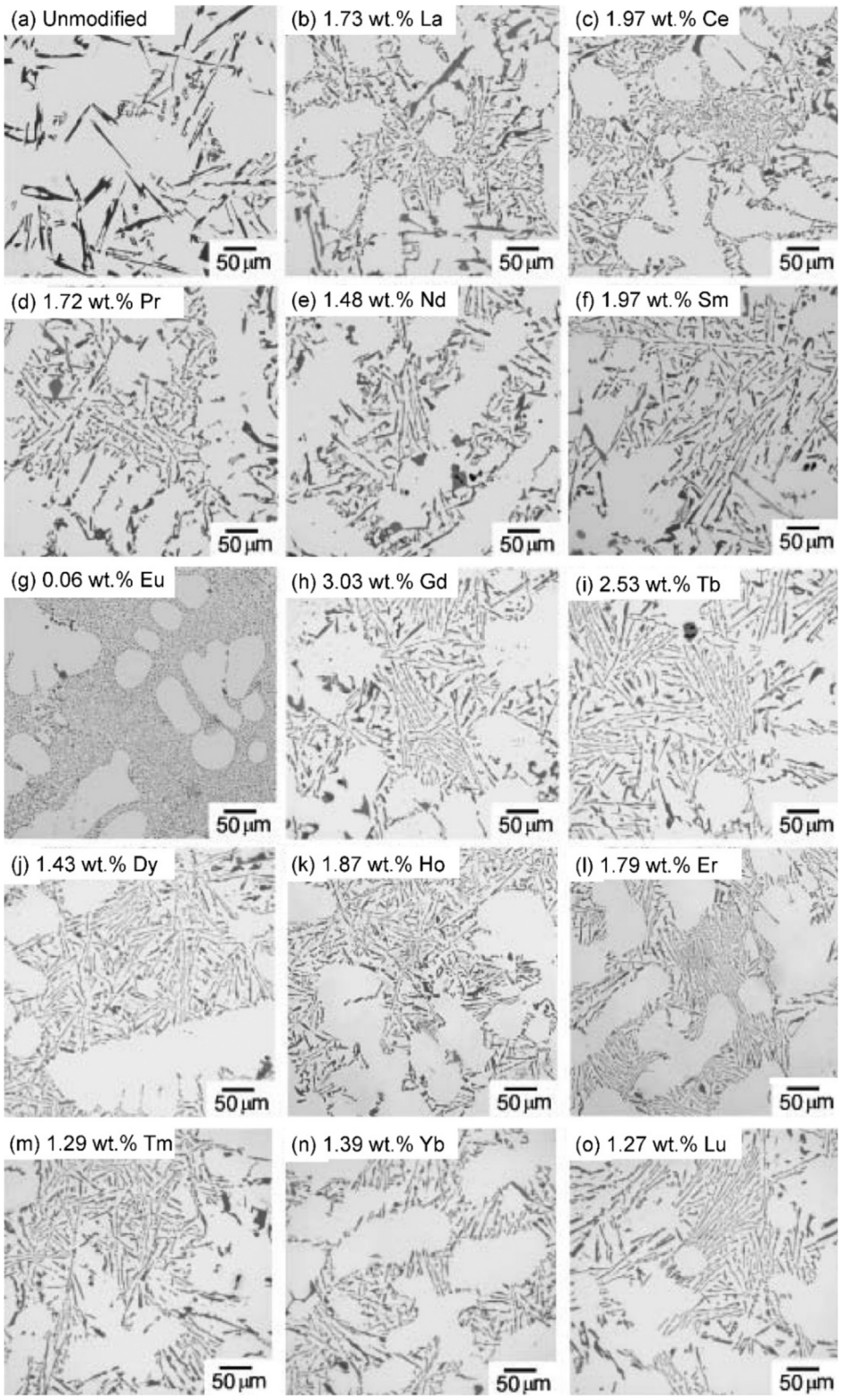

Fig. 16 – Microstructures of Al–10Si alloy at the addition level (wt.%) corresponding to the fully modified structure for the specified lanthanides.
Reproduced with permission from Ref. [91]. Copyright (2004), J-Stage.

fraction of these compounds increases with the increasing amount of lanthanide [94]. $Al_2La_5Si_2$, $Al_2Ce_5Si_2$, Al_2LaSi, Al_2CeSi, AlLaSi, $Al_4Ce_3Si_2$ and $Al_5La_3Si_2$ phases were detected in the form of ~1.5 μm thick plate-like or star-like particles in La- or Ce-modified Al–Si alloys [67,89,94–97]. At the same time, $Al_{12}La_3Ti_2$, $Al_9La_4Cu_2Si_4$, $Al_{21}Ti_2La$, $Al_{21}Ti_2Ce$,

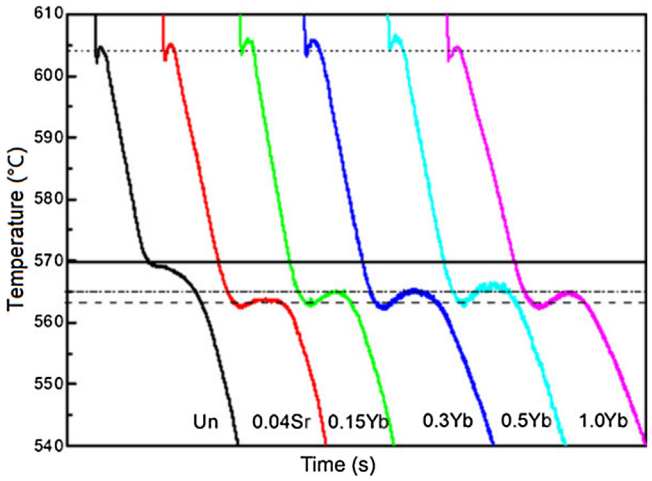

Fig. 17 – Cooling curves of A356 alloy after Yb additions; unmodified and Sr-modified alloys are illustrated as references.
Reproduced with permission from Ref. [98]. Copyright (2011), Elsevier.

$Al_{11}La_3(Cu, Fe)_4Si_2$, $Al_{11}Ce_3(Cu, Fe)_4Si_2$ and $Al_5CuSi_2La_2$ intermetallics would precipitate when the alloy contains Cu, Ti, Sr or Fe, which have a high affinity to react with lanthanides. Among these elements, Fe shows the lowest tendency to react with lanthanides [95].

No relations between silicon morphology and eutectic nucleation or growth temperatures have been observed in modified hypoeutectic Al–Si alloys. Fig. 17 shows that depressions in nucleation and growth temperatures are almost the same after Sr and Yb additions. However, the finest modification was obtained at 0.3 wt.% Yb addition, according to metallographic investigations [98].

Although almost all of the lanthanides are within the ideal range of radius ratio r_i/r for eutectic Si modification as provided by Lu et al. [35], they behave differently. All lanthanides (except Pm) could be modifiers, but Eu is the only lanthanide that can perfectly modify the eutectic Si phase and increase Si twin density [5,91]. Therefore, it should be noted that the modification mechanism of lanthanides is still undetermined and must be developed. The atomic ratio r_i/r approach based on the geometrical approach of the IIT mechanism is not sufficient to explain some behaviours and characteristics.

The privilege performance of Eu may be due to its Gibbs energy for oxidation. Europium has the highest Gibbs energy for oxidation among the lanthanides and it is −1041 kJ/g mol O_2, which is higher than that of Al_2O_3 (Fig. 6). In this case, the oxidation tendency of aluminium is higher than that of europium. All other lanthanides have quite low Gibbs energy for oxidation. Although La, Ce, Nd and Yb have relatively high Gibbs energy, their Gibbs energies are lower than that of aluminium considerably. Erbium has the highest tendency for oxidation. The stability of Er is unveiled due to differences between nominal and actual erbium ratios during addition. Despite the argon atmosphere, erbium losing is about 25% in molten aluminium after 30 min [76].

5.4.1. *Future opportunities of lanthanides*

To achieve a fully modified structure in Al–7Si type alloys, a minimum of 3000 ppm lanthanide addition is necessary, and this level increases with increasing Si ratio. On the other side, about 200 ppm Sr is generally enough to achieve the same performance.

Global resources of strontium and all lanthanides are more than 1 billion t and 410 million t, respectively [2,10]. Considering that all these resources were used in eutectic Si modification, it would be possible to chemically modify 4000 billion t of molten aluminium alloys with Sr resources; on the other side, only 137 billion t could be modified by lanthanides' addition.

The actual cost and efficiency make lanthanides still far to be individually used in foundry world for commercial and widespread applications. Future research could work on the synergy among lanthanides for an effective eutectic silicon modification in hypoeutectic Al–Si alloys. Definitely, if a better modification performance occurred by a kind of multiple addition of several lanthanides in lower ratios, such as 30 ppm each, then the use of lanthanides could be convenient economically.

Several studies [67,94,97,99,100] show no remarkable difference between the effects of La-based or Ce-based mischmetals (usually La, Ce, Nd, Y) on the microstructure and mechanical properties of hypoeutectic Al–Si alloys; this is due to the chemical similarity of both these elements. In these terms, the supply to foundry is facilitated due to the variety of products. However, in order to increase the effectiveness of mischmetal on eutectic modification, a new generation of mischmetals should be studied where a mixture of different lanthanide elements might be used.

Future works must be focused on silicon modification with combined additions of lanthanides and their effects. New generations of lanthanides-containing master alloys could be thus appeared in the market for eutectic Si modification.

6. Conclusions

Eutectic modification plays important role to improve the whole properties of Al–Si foundry alloys by nucleating the eutectic grains heterogeneously and by changing the morphology of eutectic silicon. Nowadays, several researches have paid attention on lanthanides, which seem to be a possible alternative to commercial eutectic modifiers, such as Na and Sr. A better modification level obtained with less addition amounts is expected by these elements of the group IIIB of the periodic table. However, when about 200 ppm Sr addition is enough for good eutectic modification and activating twinning mechanism in hypoeutectic Al–Si alloys, most of the lanthanides need 3000 ppm additions for eutectic silicon refinement in the same casting alloys.

Lanthanide elements (except Eu) are ineffective to modify the eutectic silicon. They can only refine the plate-like morphology even at the high amount of addition (>1 wt.% of lanthanide) and this behaviour is dissimilar to that of Sr and Na.

La, Ce and Nd, the most preferred lanthanide elements in the metallurgy industry due to the mischmetal demand of the

foundries, cannot fully modify the eutectic structure, although their relatively great abundance in the Earth's crust and low prices.

High content of lanthanides in the alloy and the presence of Cu, Ti, Sr, or Fe alloying elements cause the formation of a large number of lanthanide-rich complex intermetallics and oxides. The increasing content of lanthanide enhances the volume fraction of these compounds, which can hinder the liquid flow during solidification leading to greater porosity in the alloy.

Among lanthanides, Eu appears to be the only one element in this group that can lead to a fully modified eutectic structure in hypoeutectic Al–Si alloys.

Conflicts of interest

The authors declare no conflict of interest.

Acknowledgements

The work was developed with the financial support of Fondazione Cassa di Risparmio di Padova e Rovigo (CariPaRo), Padova (2019).

REFERENCES

[1] Klinger JM. A historical geography of rare earth elements: from discovery to the atomic age. Extract Ind Soc 2015;2(3):572–80, http://dx.doi.org/10.1016/j.exis.2015.05.006.
[2] Zhou B, Li Z, Chen C. Global potential of rare earth resources and rare earth demand from clean technologies. Minerals 2017;7(11):203, http://dx.doi.org/10.3390/min7110203.
[3] Goonan TG. Rare earth elements – end use and recyclability. In: U.S. geological survey scientific investigations. Report 2011-5094; 2011, 15 p., Available from: http://pubs.usgs.gov/sir/2011/5094/.
[4] Seddon M. Rare earth market overview. London, England: Argus Media Ltd; 2019. Available from: http://www.argusjapan.com/cgi-bin/MetalsForum2018/RareEarths_ArgusMetalForum.pdf [accessed 10.05.20].
[5] Moniri S, Shahani AJ. Chemical modification of degenerate eutectics: a review of recent advances and current issues. J Mater Res 2019;34(1):20–34, http://dx.doi.org/10.1557/jmr.2018.361.
[6] Henderson P, editor. Rare earth element geochemistry. Elsevier; 2013. ISBN: 0-444-42148-3.
[7] Lucas J, Lucas P, Le Mercier T, Rollat A, Davenport WG. Rare earths: science, technology, production and use. Elsevier; 2014. ISBN: 978-0-444-62735-3.
[8] Haynes WM. CRC handbook of chemistry and physics. CRC press; 2014. ISBN: 978-1-4822-0868-9.
[9] Hurst C. China's rare earth elements industry: what can the west learn? Washington DC: Institute for the Analysis of Global Security; 2010. Available from: https://apps.dtic.mil/docs/citations/ADA525378 [accessed 19.03.20].
[10] Bernhardt D, Reilly J. Mineral commodity summaries 2020. Reston, USA: US Geological Survey; 2020. Available from: https://www.usgs.gov/centers/nmic/mineral-commodity-summaries [accessed 01.05.20].
[11] De Lima IB, Leal Filho W, editors. Rare earths industry: technological, economic, and environmental implications. Elsevier; 2015. ISBN: 978-0-12-802328-0.
[12] Salazar K, McNutt MK. Metal prices in the United States through 2010. Reston, Virginia: US Geological Survey; 2013. Available from: https://pubs.usgs.gov/sir/2012/5188/ [accessed 19.03.20].
[13] Fernandez V. Rare-earth elements market: a historical and financial perspective. Resour Policy 2017;53:26–45, http://dx.doi.org/10.1016/j.resourpol.2017.05.010.
[14] Mae Y. Schematic interpretation of anomalies in the physical properties of Eu and Yb among the lanthanides. Int J Mater Sci Appl 2017;64:165–70, http://dx.doi.org/10.11648/j.ijmsa.20170604.11.
[15] Gschneidner KA Jr, Daane AH. Physical metallurgy. Handb Phys Chem Rare Earths 1988;11:409–84, http://dx.doi.org/10.1016/S0168-1273(88)11010-6.
[16] Krishnamurthy N, Gupta CK. Extractive metallurgy of rare earths. CRC Press; 2015. ISBN: 978-1-4665-7638-4.
[17] Awadh B. Pandey: direct forging and rolling of L12 aluminum alloys for armor applications. US Patent US9127334B2; 2009.
[18] International ASM. Alloy phase diagram, vol 10. 10.1007/BF02881433; 1989.
[19] Okamoto H. Al–Sm (aluminium–samarium). J Phase Equilib diffus 2012;33(3):243, http://dx.doi.org/10.1007/s11669-012-0019-y.
[20] Nogita K, Yasuda H, Yoshiya M, McDonald SD, Uesugi K, Takeuchi A, et al. The role of trace element segregation in the eutectic modification of hypoeutectic Al–Si alloys. J Alloys Compd 2010;489(2):415–20, http://dx.doi.org/10.1016/j.jallcom.2009.09.138.
[21] Okamoto H. Phase diagram updates. J Phase Equilib 1991;12(4):499, http://dx.doi.org/10.1007/BF02645980.
[22] Okamoto H. Al–Er (aluminum–erbium). J Phase Equilib Diffus 2011;32(3):261, http://dx.doi.org/10.1007/s11669-011-9877-y.
[23] Okamoto H. Al–La (aluminum–lanthanum). J Phase Equilib Diffus 2007;28(6):581, http://dx.doi.org/10.1007/s11669-007.
[24] Okamoto H. Supplemental literature review of binary phase diagrams: Al–Bi, Al–Dy, Al–Gd, Al–Tb, C–Mn, Co–Ga, Cr–Hf, Cr–Na, Er–H, Er–Zr, H–Zr, and Ni–Pb. J Phase Equilib Diffus 2014;35(3):343–54, http://dx.doi.org/10.1007/s11669-014-0300-3.
[25] Ho CR, Cantor B. Heterogeneous nucleation of solidification of Si in Al–Si and Al–Si–P alloys. Acta Metall Mater 1995;43(8):3231–46, http://dx.doi.org/10.1016/0956-7151(94)00480-6.
[26] Ho CR, Cantor B. Heterogeneous nucleation of solidification of Si in Al–Si. Mater Sci Eng A 1993;173(1-2):37–40, http://dx.doi.org/10.1016/0921-5093(93)90182-E.
[27] Cantor B. Impurity effects on heterogeneous nucleation. Mater Sci Eng A 1997;226:151–6, http://dx.doi.org/10.1016/S0921-5093(96)10608-0.
[28] Zhang DL, Cantor B. Heterogeneous nucleation of solidification of Si by solid AI in hypoeutectic Al–Si alloy. Metall Trans A 1993;24(5):1195–204, http://dx.doi.org/10.1007/BF02657251.
[29] Shankar S, Riddle YW, Makhlouf MM. Nucleation mechanism of the eutectic phases in aluminum–silicon hypoeutectic alloys. Acta Mater 2004;52(15):4447–60, http://dx.doi.org/10.1016/j.actamat.2004.05.045.
[30] Cho YH, Lee HC, Oh KH, Dahle AK. Effect of strontium and phosphorus on eutectic Al–Si nucleation and formation of β-Al 5 FeSi in hypoeutectic Al–Si foundry alloys. Metall Mater Trans A 2008;39(10):2435–48, http://dx.doi.org/10.1007/s11661-008-9580-8.

[31] Ludwig TH, Dæhlen ES, Schaffer PL, Arnberg L. The effect of Ca and P interaction on the Al–Si eutectic in a hypoeutectic Al–Si alloy. J Alloys Compd 2014;586:180–90, http://dx.doi.org/10.1016/j.jallcom.2013.09.127.
[32] Campbell J, Tiryakioğlu M. Review of effect of P and Sr on modification and porosity development in Al–Si alloys. Mater Sci Technol 2010;263:262–8, http://dx.doi.org/10.1179/174328409X425227.
[33] Sigworth G, Campbell J, Jorstad J. The modification of Al–Si casting alloys: important practical and theoretical aspects. Int J Metalcast 2009;3(1):65–78, http://dx.doi.org/10.1007/BF03355442.
[34] Campbell J. Complete casting handbook: metal casting processes, metallurgy, techniques and design. 2nd ed. Butterworth-Heinemann; 2015. p. 245. ISBN: 978-0-444-63509-9.
[35] Lu SZ, Hellawell A. The mechanism of silicon modification in aluminium–silicon alloys: impurity induced twinning. Metall Trans A 1987;18(10):1721–33, http://dx.doi.org/10.1007/BF02646204.
[36] Khan S, Elliott R. Quench modification of aluminium–silicon eutectic alloys. J Mater Sci 1996;31(14):3731–7, http://dx.doi.org/10.1007/BF00352787.
[37] Di Giovanni MT, de Menezes JT, Cerri E, Castrodeza EM. Influence of microstructure and porosity on the fracture toughness of Al–Si–Mg alloy. J Mater Res Technol 2019, http://dx.doi.org/10.1016/j.jmrt.2019.11.055 [In press].
[38] Pacz A. Alloy. US Patent US1387900A; 1921.
[39] Engstler M, Barrirero J, Ghafoor N, Odén M, Mücklich F. 3D microstructure characterization and analysis of Al–Si foundry alloys at different length scales. Microsc Microanal 2014;20(S3):956–7, http://dx.doi.org/10.1017/S1431927614006503.
[40] McDonald SD, Nogita K, Dahle AK. Eutectic nucleation in Al–Si alloys. Acta Mater 2004;52(14):4273–80, http://dx.doi.org/10.1016/j.actamat.2004.05.043.
[41] Tsumura Y. On the theory of modification of aluminium-silicon alloys. J Jpn Inst Met Mater 1957;21(2):69–83, http://dx.doi.org/10.2320/jinstmet1952.21.2_69.
[42] Day MG, Hellawell A. The microstructure and crystallography of aluminium–silicon eutectic alloys. Proc R Soc Lond Ser A Math Phys Sci 1968;305(1483):473–91, http://dx.doi.org/10.1098/rspa.1968.0128.
[43] Nogita K, Knuutine A, McDonald SD, Dahle AK. Mechanisms of eutectic solidification in Al–Si alloys modified with Ba, Ca, Y and Yb. J Light Met 2001;1(4):219–28, http://dx.doi.org/10.1016/S1471-5317(02)00005-6.
[44] McDonald SD. Eutectic solidification and porosity formation in unmodified and modified hypoeutectic aluminium-silicon alloys. University of Queensland; 2002. p. 171–3 [PhD thesis].
[45] Li JH, Zarif MZ, Albu M, McKay BJ, Hofer F, Schumacher P. Nucleation kinetics of entrained eutectic Si in Al–5Si alloys. Acta Mater 2014;72:80–98, http://dx.doi.org/10.1016/j.actamat.2014.03.030.
[46] Li JH, Albu M, Hofer F, Schumacher P. Solute adsorption and entrapment during eutectic Si growth in A–Si-based alloys. Acta Mater 2015;83:187–202, http://dx.doi.org/10.1016/j.actamat.2014.09.040.
[47] Lu L, Nogita K, Dahle AK. Combining Sr and Na additions in hypoeutectic Al–Si foundry alloys. Mater Sci Eng A 2005;399(1-2):244–53, http://dx.doi.org/10.1016/j.msea.2005.03.091.
[48] Cardinale AM, Macciò D, Saccone A. Phase equilibria of the Dy–Al–Si system at 500 °C. J Therm Anal Calorim 2012;108(2):817–23, http://dx.doi.org/10.1007/s10973-012-2196-7.
[49] Cardinale AM, Parodi N. Tb–Al–Si systems. J Therm Anal Calorim 2019;138(3):2057–64, http://dx.doi.org/10.1007/s10973-019-08500-5.
[50] Gröbner J, Mirković D, Schmid-Fetzer R. Thermodynamic aspects of the constitution, grain refining, and solidification enthalpies of Al–Ce–Si alloys. Metall Mater Trans A 2004;35(11):3349–62, http://dx.doi.org/10.1007/s11661-004-0172-y.
[51] Cardinale AM, Macciò D, Saccone A. Phase equilibria in the Sm–Al–Si system at 500 °C. J Therm Anal Calorim 2014;116(1):61–7, http://dx.doi.org/10.1007/s10973-014-3722.-6.
[52] Cardinale AM, Parodi N. The Gd–Al–Si isothermal section at 500 °C. J Phase Equilib Diffus 2018;39(1):68–73, http://dx.doi.org/10.1007/s11669-017-0608-x.
[53] Cardinale AM, Parod N. R–Al–Si systems (R: Pr, Nd). J Therm Anal Calorim 2018;134(2):1327–35, http://dx.doi.org/10.1007/s10973-018-7536-9.
[54] Samarium and/or gadolinium-containing heat-resisting cast aluminum alloy and preparation method thereof. China CN104294109A; 2014.
[55] High-toughness cast aluminum-silicon alloy and preparation method and application thereof. China CN109338180B; 2018.
[56] Patent: Masumoto T.: High strength, heat-resistant aluminum-based alloys. US Patent 5053085A, 1993.
[57] Al–Si–Mg–Sm rare earth cast aluminum alloy and preparation method thereof. China CN102758108A; 2012.
[58] High-strength heat-proof aluminum alloy material containing beryllium and rare earth and producing method thereof. WIPO (PCT) WO2011035654A1; 2009.
[59] Abdelaziz MH, Samuel AM, Doty HW, Valtierra S, Samuel FH. Effect of additives on the microstructure and tensile properties of Al–Si alloys. J Mater Res Technol 2019;8(2):2255–68, http://dx.doi.org/10.1016/j.jmrt.2019.03.003.
[60] De Giovanni M, Kaduk JA, Srirangam P. Modification of Al–Si Alloys by Ce or Ce with Sr. JOM 2019;71(1):426–34, http://dx.doi.org/10.1007/s11837-018-3192-6.
[61] Tsai YC, Chou CY, Lee SL, Lin CK, Lin JC, Lim SW. Effect of trace La addition on the microstructures and mechanical properties of A356 (Al–7Si–0.35 Mg) aluminum alloys. J Alloys Compd 2009;487(1-2):157–62, http://dx.doi.org/10.1016/j.jallcom.2009.07.183.
[62] Tsai YC, Chou CY, Jeng RR, Lee SL, Lin CK. Effect of rare earth elements addition on microstructures and mechanical properties of A356 alloy. Int J Cast Met Res 2011;24(2):83–7, http://dx.doi.org/10.1179/136404610X12816241546456.
[63] Tsai YC, Lee SL, Lin CK. Effect of trace Ce addition on the microstructures and mechanical properties of A356 (AL–7SI–0.35 Mg) aluminum alloys. J Chin Inst Eng 2011;345:609–16, http://dx.doi.org/10.1080/02533839.2011.577598.
[64] Vijayan V, Prabhu KN. The effect of simultaneous refinement and modification by cerium on microstructure and mechanical properties of Al–8% Si alloy. Int J Cast Met Res 2016;29(6):345–9, http://dx.doi.org/10.1080/13640461.2016.1144698.
[65] Niu G, Mao J, Wang J. Effect of Ce addition on fluidity of casting aluminum alloy A356. Metall Mater Trans A 2019;50(12):5935–44, http://dx.doi.org/10.1007/s11661-019-05458-9.
[66] Zhu M, Jian Z, Yao L, Liu C, Yang G, Zhou Y. Effect of mischmetal modification treatment on the microstructure, tensile properties, and fracture behavior of Al–7.0% Si–0.3% Mg foundry aluminum alloys. J Mater Sci 2011;46(8):2685–94, http://dx.doi.org/10.1007/s10853-010-5135-7.

[67] Mahmoud MG, Elgallad EM, Ibrahim MF, Samuel FH. Effect of rare earth metals on porosity formation in A356 alloy. Int J Metalcast 2018;12(2):251–65, http://dx.doi.org/10.1007/s40962-017-0156-5.
[68] Qiu H, Yan H, Hu Z. Effect of samarium (Sm) addition on the microstructures and mechanical properties of Al–7Si–0.7 Mg alloys. J Alloys Compd 2013;567:77–81, http://dx.doi.org/10.1016/j.jallcom.2013.03.050.
[69] Qiu H, Yan H, Hu Z. Modification of near-eutectic Al–Si alloys with rare earth element samarium. J Mater Res 2014;29(11):1270–7, http://dx.doi.org/10.1557/jmr.2014113.
[70] Mao F, Yan G, Xuan Z, Cao Z, Wang T. Effect of Eu addition on the microstructures and mechanical properties of A356 aluminum alloys. J Alloys Compd 2015;650:896–906, http://dx.doi.org/10.1016/j.jallcom.2015.06.266.
[71] Li JH, Wang XD, Ludwig TH, Tsunekawa Y, Arnberg L, Jiang JZ, et al. Modification of eutectic Si in Al–Si alloys with Eu addition. Acta Mater 2015;84:153–63, http://dx.doi.org/10.1016/j.actamat.2014.10.064.
[72] Li JH, Ludwig TH, Oberdorfer B, Schumacher P. Solidification behaviour of Al–Si based alloys with controlled additions of Eu and P. Int J Cast Met Res 2018;31(6):319–31, http://dx.doi.org/10.1080/13640461.2018.1480891.
[73] Shi Z, Wang Q, Shi Y, Zhao G, Zhang R. Microstructure and mechanical properties of Gd-modified A356 aluminum alloys. J Rare Earths 2015;33(9):1004–9, http://dx.doi.org/10.1016/S1002-0721(14)60518-4.
[74] Liu W, Xiao W, Xu C, Liu M, Ma C. Synergistic effects of Gd and Zr on grain refinement and eutectic Si modification of Al–Si cast alloy. Mater Sci Eng A 2017;693:93–100, http://dx.doi.org/10.1016/j.msea.2017.03.097.
[75] Wang Q, Shi Z, Li H, Lin Y, Li N, Zhao G, et al. Effects of holmium additions on microstructure and properties of A356 aluminum alloys. Metals 2018;8(10):849, http://dx.doi.org/10.3390/met8100849.
[76] Colombo M, Gariboldi E, Morri A. Er addition to Al–Si–Mg-based casting alloy: effects on microstructure, room and high temperature mechanical properties. J Alloys Compd 2017;708:1234–44, http://dx.doi.org/10.1016/j.jallcom.2017.03.076.
[77] Colombo M, Albu M, Gariboldi E, Hofer F. Microstructural changes induced by Er and Zr additions to A356 alloy investigated by thermal analyses and STEM observations. Mater Charact 2020;161:110117, http://dx.doi.org/10.1016/j.matchar.2020.110117.
[78] Hu X, Jiang F, Ai F, Yan H. Effects of rare earth Er additions on microstructure development and mechanical properties of die-cast ADC12 aluminum alloy. J Alloys Compd 2012;538:21–7, http://dx.doi.org/10.1016/j.jallcom.2012.05.089.
[79] Al–Si–Mg–Er rare earth casting aluminium alloy. China CN101705397A; 2009.
[80] Pengfei X, Bo GAO, Zhuang Y, Kaihua L, Ganfeng TU. Effect of erbium on properties and microstructure of Al–Si eutectic alloy. J Rare Earths 2010;28(6):927–30, http://dx.doi.org/10.1016/S1002-0721(09)60222-2.
[81] Jia K, Yu WB, Yao JM, Zhang S, Wu H. Al–9.00% Si–0.25% Mg alloys modified by ytterbium. Rare Met 2017;36(2):95–100, http://dx.doi.org/10.1007/s12598-014-0378-0.
[82] Hu Z, Dong Z, Yin Z, Yan H, Tian J, Xie H. Solidification behavior, microstructure and silicon twinning of Al–10Si alloys with ytterbium addition. J Rare Earths 2018;36(6):662–8, http://dx.doi.org/10.1016/j.jre.2017.12.007.
[83] Li JH, Suetsugu S, Tsunekawa Y, Schumacher P. Refinement of eutectic Si phase in Al–5Si alloys with Yb additions. Metall Mater Trans A 2013;44(2):669–81, http://dx.doi.org/10.1007/s11661-012-1410-3.
[84] Hegde S, Prabhu K. N. Modification of eutectic silicon in Al–Si alloys. J Mater Sci 2008;43(9):3009–27, http://dx.doi.org/10.1007/s10853-008-2505-5.
[85] Li L, Li D, Mao F, Feng J, Zhang Y, Kang Y. Effect of cooling rate on eutectic Si in Al–7.0 Si–0.3 Mg alloys modified by La additions. J Alloys Compd 2020;826:154206, http://dx.doi.org/10.1016/j.jallcom.2020.154206.
[86] Shabestari SG, Shahri F. Influence of modification, solidification conditions and heat treatment on the microstructure and mechanical properties of A356 aluminum alloy. J Mater Sci 2004;39(6):2023–32, http://dx.doi.org/10.1023/B:JMSC. 0000017764.20609.0d.
[87] Knuutinen A, Nogita K, McDonald SD, Dahle AK. Porosity formation in aluminium alloy A356 modified with Ba, Ca, Y and Yb. J Light Met 2001;1(4):241–9, http://dx.doi.org/10.1016/S1471-5317(02)00006-8.
[88] Zhang X, Wang Z, Zhou Z, Xu J. Influence of rare earth (Ce and La) addition on the performance of Al–3.0 wt% Mg alloy. J Wuhan Univ Technology Mater Sci Ed 2017;32(3):611–8, http://dx.doi.org/10.1007/s11595-017-1642-6.
[89] Mahmoud MG, Samuel AM, Doty HW, Samuel FH. Effect of the addition of La and Ce on the solidification behavior of Al–Cu and Al–Si–Cu cast alloys. Int J Metalcast 2020;14(1):191–206, http://dx.doi.org/10.1007/s40962-019-00351-y.
[90] Jing L, Pan Y, Lu T, Chai W. Refinement effect of two rare earth borides in an Al–7Si–4Cu alloy: a comparative study. Mater Charact 2018;145:664–70, http://dx.doi.org/10.1016/j.matchar.2018.09.031.
[91] Nogita K, McDonald SD, Dahle AK. Eutectic modification of Al–Si alloys with rare earth metals. Mater Trans 2004;45(2):323–6, http://dx.doi.org/10.2320/matertrans.45.323.
[92] Nogita K, Drennan J, Dahle AK. Evaluation of silicon twinning in hypo-eutectic Al–Si alloys. Mater Trans 2003;44(4):625–8, http://dx.doi.org/10.2320/matertrans.44.625.
[93] Mahmoud MG, Samuel AM, Doty HW, Samuel FH. Role of heat treatment on the tensile properties and fractography of Al–1.2 Si–2.4 Cu and Al–8.0 Si–2.4 Cu cast alloys modified with Ce, La and Sr addition. Int J Metalcast 2020;14(1):218–42, http://dx.doi.org/10.1007/s40962-019-00350-z.
[94] Mahmoud MG, Samuel AM, Doty HW, Samuel FH. Formation of rare earth intermetallics in Al–Cu Cast alloys. In: Light metal symposium held at the 149th annual meeting and exhibition. Proceedings of TMS: 2020, February 23–27. 2020. p. 241–6, http://dx.doi.org/10.1007/978-3-030-36408-3_34.
[95] Samuel AM, Doty HW, Valtierra S, Samuel FH. Intermetallic precipitation in rare earth-treated A413.1 alloy: a metallographic study. Int J Mater Res 2018;109(2):157–71, http://dx.doi.org/10.3139/146.111591.
[96] Samuel AM, Elgallad EM, Mahmoud MG, Doty HW, Valtierra S, Samuel FH. Rare earth metal-based intermetallics formation in Al–Cu–Mg and Al–Si–Cu–Mg alloys: a metallographic study. Adv Mater Sci Eng 2018, http://dx.doi.org/10.1155/2018/7607465.
[97] Mahmoud MG, Samuel AM, Doty HW, Valtierra S, Samuel FH. Effect of rare earth metals, Sr, and Ti addition on the microstructural characterization of A413. 1 alloy. Adv Mater Sci Eng 2017:12, http://dx.doi.org/10.1155/2017/4712946.
[98] Li B, Wang H, Jie J, Wei Z. Microstructure evolution and modification mechanism of the ytterbium modified Al–7.5% Si–0.45% Mg alloys. J Alloys Compd 2011;509(7):3387–92, http://dx.doi.org/10.1016/j.jallcom.2010.12.081.
[99] Sims ZC, Weiss D, Rios O, Henderson HB, Kesler MS, McCall SK, et al. The efficacy of replacing metallic cerium in aluminum–cerium alloys with LREE mischmetal. In: Light

metal symposium held at the 149th annual meeting and exhibition. Proceedings of TMS: 2020, February 23–27. 2020. p. 216–21, http://dx.doi.org/10.1007/978-3-030-36408-3_30.
[100] Tash M, Khalifa W, El-Mahallawi I. Thermal analysis and microstructure of Al–12% Si–2.5% Cu–0.4% Mg cast alloy with Ce and/or La rare earth metals. In: Light metal symposium held at the 149th annual meeting and exhibition. Proceedings of TMS: 2020 February 23–27. 2020. p. 1056–62, http://dx.doi.org/10.1007/978-3-030-36408-3_144.